UNCLASSIFIED

AD NUMBER
ADB805965

CLASSIFICATION CHANGES

TO:	unclassified
FROM:	restricted

LIMITATION CHANGES

TO:

Approved for public release; distribution is unlimited.

FROM:

Distribution authorized to DoD only; Administrative/Operational Use; APR 1947. Other requests shall be referred to National Aeronautics and Space Administration, Washington, DC. Pre-dates formal DoD distribution statements. Treat as DoD only.

AUTHORITY

E.O. 10501 dtd 5 Nov 1953; NASA TR Server website

THIS PAGE IS UNCLASSIFIED

NATIONAL ADVISORY COMMITTEE
FOR AERONAUTICS

TECHNICAL NOTE

No. 1113

COLLECTION AND ANALYSIS OF HINGE-MOMENT DATA

ON CONTROL-SURFACE TABS

By Paul E. Purser and Charles B. Cook

Langley Memorial Aeronautical Laboratory
Langley Field, Va.

Washington

April 1947

NATIONAL ADVISORY COMMITTEE FOR AERONAUTICS

TECHNICAL NOTE NO. 1113

COLLECTION AND ANALYSIS OF HINGE-MOMENT DATA

ON CONTROL-SURFACE TABS

By Paul E. Purser and Charles B. Cook

SUMMARY

Various wind-tunnel data on the hinge-moment charac-
teristics of control-surface tabs have been collected and
analyzed. The data, all of which are for plain unbalanced
tabs, were obtained from force tests of models in two-
and three-dimensional flow and from pressure-distribution
measurements on models in two-dimensional flow. Some data
that show the effects of Mach number on tab hinge moments
for representative conventional and NACA 6-series airfoil
sections are presented.

The analysis indicated that present methods of esti-
mating the section values of the slope of the curves of
control-surface hinge moment plotted against angle of
attack $c_{h_{f_\alpha}}$ and against control-surface deflection $c_{h_{f_{\delta_f}}}$
over small ranges of angle of attack and deflection could
be extended to chord ratios small enough to include the
slope of the curve of tab hinge moment plotted against
angle of attack $c_{h_{t_\alpha}}$. Sufficient data were not available
to extend the analysis to include the slope of the curve
of tab hinge moment against tab deflection $c_{h_{t_{\delta_t}}}$, but
such an extension should be possible when more tab data
are available. The values of the slope of the curve of
tab hinge moment plotted against control-surface deflec-
tion $c_{h_{t_{\delta_f}}}$ were found to depend upon the ratio of tab
chord to control-surface chord c_t/c_f, upon the ratio of
control-surface chord to airfoil chord c_f/c, upon the
control-surface trailing-edge angle $\emptyset$, and upon the

condition of the gaps at the tab and control-surface hinge
lines. An analysis of approximate aspect-ratio correc-
tions (derived from lifting-line theory) for correcting
the section values of $ch_{t_{\delta_f}}$ to finite-span values indi-
cated that the correction depended upon c_f/c and c_t/c_f
as well as upon aspect ratio.

The data available were not sufficient to allow accu-
rate determinations of all the various factors affecting
the differences between section and finite-span values of
the tab hinge-moment parameters; thus the desirability of
obtaining more tab hinge-moment data on finite-span models
at larger values of Mach number and of obtaining more
complete aspect-ratio corrections to tab hinge-moment
characteristics is indicated.

INTRODUCTION

In an effort to provide satisfactory methods for
predicting control-surface characteristics, the NACA has
undertaken a program of summarizing, analyzing, and corre-
lating the results of various experimental investigations
of airplane control surfaces. This program has provided
collections of aileron and tail-surface test data (refer-
ences 1 and 2), analyses and correlations of the hinge-
moment characteristics of control surfaces with internal
balances, plain-overhang and Frise balances, beveled
trailing edges, shielded and unshielded horn balances and
tabs (references 3 to 8), and an analysis of the lift
effectiveness of control surfaces (reference 9).

As airplane sizes and speeds increase and as more
reliance is placed upon tabs (particularly spring-linked
tabs) to provide the final adjustment of control forces,
the hinge moment of the tab about its own hinge axis
becomes increasingly important. (See references 10 and 11.)
The present report therefore presents an analysis and
correlation of the available data on tab hinge-moment
characteristics.

COEFFICIENTS AND SYMBOLS

c_l airfoil section lift coefficient (l/qc)

c_{h_f} flap section hinge-moment coefficient $\left(h_f/qc_f{}^2\right)$

C_{h_f} flap hinge-moment coefficient $\left(H_f/qb_f\bar{c}_f{}^2\right)$

c_{h_t} tab section hinge-moment coefficient $\left(h_t/qc_t{}^2\right)$

C_{h_t} tab hinge-moment coefficient $\left(H_t/qb_t\bar{c}_t{}^2\right)$

P_R resultant pressure coefficient $\left(\dfrac{p_L - p_U}{q}\right)$

where

l airfoil section lift

h_f flap section hinge moment

H_f flap hinge moment

h_t tab section hinge moment

H_t tab hinge moment

q free-stream dynamic pressure

c airfoil section chord

c_f flap section chord behind hinge line

$\bar{c}_f$ root-mean-square flap chord behind hinge line

c_t tab section chord behind hinge line

$\bar{c}_t$ root-mean-square tab chord behind hinge line

b_f flap span

b_t tab span

p_U static pressure on upper surface of airfoil

p_L static pressure on lower surface of airfoil

$\overline{c}_f{}'$ root-mean-square chord of portion of flap spanned by tab

a_0 angle of attack for infinite aspect ratio, degrees

a angle of attack, degrees

δ_f deflection of flap with respect to airfoil, degrees

δ_t deflection of tab with respect to flap, degrees

$\emptyset$ trailing-edge angle, angle included between upper and lower surfaces at airfoil trailing edge, degrees

A aspect ratio (b^2/s)

E Jones' edge-velocity factor (reference 12)

λ taper ratio $\left(\dfrac{\text{Tip chord}}{\text{Root chord}}\right)$

k section tab hinge-moment constant

K finite-span tab hinge-moment constant

x chordwise location of pressure vent measured from airfoil nose

τ turbulence factor for tunnel

R Reynolds number

M Mach number

b wing span

y_i spanwise location of tab measured from wing root to inboard end of tab

y_o spanwise location of tab measured from wing root to outboard end of tab

Derivatives:

The subscripts outside of the parentheses denote the factors held constant when the derivative was taken.

$$c_{h_{f_\alpha}} = \left(\frac{\partial c_{h_f}}{\partial \alpha_o}\right)_{\delta_f, \delta_t}$$

$$C_{h_{f_\alpha}} = \left(\frac{\partial C_{h_f}}{\partial \alpha}\right)_{\delta_f, \delta_t}$$

$$c_{h_{t_\alpha}} = \left(\frac{\partial c_{h_t}}{\partial \alpha_o}\right)_{\delta_f, \delta_t}$$

$$C_{h_{t_\alpha}} = \left(\frac{\partial C_{h_t}}{\partial \alpha}\right)_{\delta_f, \delta_t}$$

$$c_{h_{f_{\delta_f}}} = \left(\frac{\partial c_{h_f}}{\partial \delta_f}\right)_{\alpha_o, \delta_t}$$

$$C_{h_{f_{\delta_f}}} = \left(\frac{\partial C_{h_f}}{\partial \delta_f}\right)_{\alpha, \delta_t}$$

$$c_{h_{t_{\delta_f}}} = \left(\frac{\partial c_{h_t}}{\partial \delta_f}\right)_{\alpha_o, \delta_t}$$

$$C_{h_{t_{\delta_f}}} = \left(\frac{\partial C_{h_t}}{\partial \delta_f}\right)_{\alpha, \delta_t}$$

$$c_{h_{t_{\delta_t}}} = \left(\frac{\partial c_{h_t}}{\partial \delta_t}\right)_{\alpha_o, \delta_f}$$

$$C_{h_{t\delta_t}} = \left(\frac{\partial C_{h_t}}{\partial \delta_t}\right)_{a,\delta_f}$$

$$P_a = \left(\frac{\partial F_R}{\partial a_o}\right)_{\delta_t,\delta_f}$$

$$P_{\delta_f} = \left(\frac{\partial P_R}{\partial \delta_f}\right)_{a_o,\delta_t}$$

$$P_{\delta_t} = \left(\frac{\partial P_R}{\partial \delta_t}\right)_{a_o,\delta_f}$$

$$a_{\delta_f} = \left(\frac{\partial a_o}{\partial \delta_f}\right)_{c_l,\delta_t}$$

$$a_{\delta_t} = \left(\frac{\partial a_o}{\partial \delta_t}\right)_{c_l,\delta_f}$$

$\Delta C_{h_{aLS}}$ lifting-surface theory correction to $C_{h_{t_a}}$
            or $C_{h_{f_a}}$

Subscript:

$(\phi = 0)$ value of the parameter at zero trailing-edge
             angle

The terms "flap" and "control surface" are used synonymously as a general expression for any movable control surface such as a rudder, elevator, or aileron.

DATA AND SCOPE

The data upon which the analysis is based were obtained from references 7 and 13 to 23, as well as from

unpublished results of tests made at the Langley and
Ames laboratories. The test conditions covered were for
models in two- and three-dimensional flow for a range of
angles of attack and flap or tab deflection of about $\pm 4^\circ$
or $\pm 5^\circ$. The geometry and other pertinent data for the
various models are summarized in tables I, II, and III.
The ranges of the various geometric parameters covered by
the models are listed in the following table:

Type test	See table	A	λ	$\emptyset$ (deg)	c_f/c	c_t/c_f	Airfoil thickness
Section pressure distribution	I	----	----	9.3 to 30.5	0.10 to 0.50	0.10 to 1.00	0.09c to 0.16c
Section force	II	----	----	7.4 to 25.0	0.18 to 0.40	0.20 to 0.75	0.09c to 0.18c
Finite-span force	III	2.41 to 6.86	1.00 to 0.39	11.5 to 16.7	0.17 to 0.41	0.20 to 0.41	0.08c to 0.18c

METHODS OF ANALYSIS

General Approach

Derivation of $c_{h_{t_\alpha}}$ and $c_{h_{t_{\delta t}}}$.- In order to deter-
mine some logical approach to the problem of correlating
tab hinge-moment characteristics, a study was made of a
previously derived analysis of $c_{h_{f_\alpha}}$ and $c_{h_{f_{\delta f}}}$ (refer-
ence 24). It was found possible to extend the analysis
of reference 24 to chord ratios small enough to include
tab hinge-moment characteristics $\left(c_{h_{t_\alpha}}$ and $c_{h_{t_{\delta t}}}\right)$.

The results of the analysis of reference 24 (which super-
sedes that of reference 5) indicated that chord ratio c_f/c
(or c_t/c) and trailing-edge angle $\emptyset$ were the primary
geometric parameters affecting $c_{h_{f_\alpha}}$ (or $c_{h_{t_\alpha}}$) and $c_{h_{f_{\delta f}}}$
(or $c_{h_{t_{\delta t}}}$). The results can be expressed by the following
formulas:

$$c_{h_f\alpha} = c_{h_f\alpha(\emptyset=0)} + \frac{dc_{h_f\alpha}}{d\emptyset} \emptyset$$

or

$$c_{h_t\alpha} = c_{h_t\alpha(\emptyset=0)} + \frac{dc_{h_t\alpha}}{d\emptyset} \emptyset \tag{1}$$

and

$$c_{h_f\delta_f} = c_{h_f\delta_f(\emptyset=0)} + \frac{dc_{h_f\delta_f}}{d\emptyset} \emptyset$$

or

$$c_{h_t\delta_t} = c_{h_t\delta_t(\emptyset=0)} + \frac{dc_{h_t\delta_t}}{d\emptyset} \emptyset \tag{2}$$

Derivation of $c_{h_t\delta_f}$.- The analysis of $c_{h_t\delta_f}$ began
with a study of values of $c_{h_t\delta_f}$ derived from the experi-
mental data of references 13 to 16 (corrected for tunnel-
wall effect) and similar data derived from Glauert's thin
airfoil theory (reference 25) as extended by Perring
(reference 26). The derivations were made by personnel
of the Langley Stability Tunnel Section for use in pre-
paring reference 27. The study indicated that a series
of straight lines would result if $c_{h_t\delta_f}$ were plotted
against $\frac{c_t}{c_f}$ with $c_{h_t\delta_f} = c_{h_f\delta_f}$ at $\frac{c_t}{c_f} = 1.0$ as the
end point. Such plots permitted derivation of the formula

$$c_{h_t\delta_f} = c_{h_f\delta_f} + k \left(1 - \frac{c_t}{c_f}\right) \tag{3}$$

where k was a constant for a given value of cf/c and
was about 10 percent lower for the experimental NACA 0009
airfoil data than for the thin-airfoil-theory data.

Specific Approach

Pressure-distribution data.- The pressure-distribution data of references 13 to 18 and unpublished data taken at the Langley Laboratory were plotted in terms of the pressure slopes P_α, $P_{\delta f}$, and $P_{\delta t}$ against pressure vent locations x/c. The plots of P_α were integrated about various chordwise axes to give values of c_{hf_α} $\left(\text{or } c_{ht_\alpha}\right)$ and plots of P_δ were integrated about the flap (or tab) hinge axes to give values of $c_{hf_{\delta f}}$ $\left(\text{or } c_{ht_{\delta t}}\right)$ for various values of c_f/c (or c_t/c). The values of c_{hf_α} $\left(\text{or } c_{ht_\alpha}\right)$ and $c_{hf_{\delta f}}$ $\left(\text{or } c_{ht_{\delta t}}\right)$ were then plotted against trailing-edge angle $\emptyset$ for the given values of c_f/c (or c_t/c) and the resulting curves extrapolated to $\emptyset = 0$ to obtain $c_{hf_{\alpha(\emptyset=0)}}$ $\left(\text{or } c_{ht_{\alpha(\emptyset=0)}}\right)$ and $c_{hf_{\delta(\emptyset=0)}}$ $\left(\text{or } c_{ht_{\delta(\emptyset=0)}}\right)$. The slopes of the curves were also measured to obtain $\dfrac{dc_{hf_\alpha}}{d\emptyset}$ $\left(\text{or } \dfrac{dc_{ht_\alpha}}{d\emptyset}\right)$ and $\dfrac{dc_{hf_{\delta f}}}{d\emptyset}$ $\left(\text{or } \dfrac{dc_{ht_{\delta t}}}{d\emptyset}\right)$.

Integration of plots of $P_{\delta f}$ about axes other than the flap hinge axis provided values of $c_{ht_{\delta f}}$ for various values of c_t/c_f for each value of c_f/c for which data were available. The resulting values of $c_{ht_{\delta f}}$ were plotted against c_t/c_f and values of k were obtained from the slopes of these curves.

Section force-test data.- The values of c_{hf_α}, c_{ht_α}, $c_{hf_{\delta f}}$, $c_{ht_{\delta t}}$, and $c_{ht_{\delta f}}$ obtained from references 19 to 23 and some unpublished data from the Langley Laboratory were used in the same way as the hinge-moment slopes derived from the pressure-distribution data. Individual values of k derived from the force-test data were more subject to error than those derived from pressure-distribution data because with force-test data there were only two test points through which to draw the line the slope of which defines k; whereas with the pressure-distribution data, as many as ten test points were sometimes available.

Finite-span data.- The finite-span data from reference 7 and some unpublished data were used to provide measured values of Cht_α and $Cht_{\delta t}$ with which to compare calculated values. The calculated values of Cht_α and $Cht_{\delta t}$ were obtained from the following empirically derived equations:

$$Cht_\alpha = \frac{A}{AE + 2} cht_{\alpha(\emptyset=0)} + \Delta Cht_{\alpha_{LS}} + \frac{\partial cht_\alpha}{\partial\emptyset} \frac{A}{A + 2} \emptyset \quad (4)$$

and

$$Cht_{\delta t} = cht_{\delta t(\emptyset=0)} + a_{\delta t(\emptyset=0)} \; cht_{\alpha(\emptyset=0)} \left(1 - \frac{A}{AE + 2}\right)$$

$$+ \frac{\partial cht_{\delta t}}{\partial\emptyset} \frac{A}{A + 2} \emptyset \quad (5)$$

where values of $\Delta Cht_{\alpha_{LS}}$ can be obtained from reference 27; $a_{\delta t(\emptyset=0)}$ can be obtained from reference 9, and the other factors can be obtained from the present report.

The finite-span data were also used to obtain values of $Chf_{\delta f}$ and $Cht_{\delta f}$ from which to derive values of K for use in the formula

$$Cht_{\delta f} = Chf_{\delta f} + K \left(1 - \overline{c}_t/\overline{c}_f'\right) \quad (6)$$

It should be noted that models 13, 14, and 16 of table III had balanced flaps. For these models $Chf_{\delta f}$ was computed by subtracting from the test data an increment in $Chf_{\delta f}$ caused by the balance as computed by use

of reference 4 for models 13 and 14 and from measured balance-chamber pressures for model 16.

So few finite-span data were available that, in an attempt to extend the usefulness of the data, aspect-ratio corrections were derived by means of lifting-line theory to permit conversion of the section k to finite-span K. The formula for the conversion was

$$K = k + \frac{\dfrac{A}{AE + 2}}{1 - \dfrac{\overline{c_t}}{\overline{c_f}'}} \, \alpha_{\delta f} \left(c_{ht_\alpha} - c_{hf_\alpha} \right) \qquad (7)$$

which indicates that K varies with aspect ratio and tab chord; whereas k varied with flap chord and trailing-edge angle. This effect of tab chord means that the curves of $C_{ht_{\delta f}}$ plotted against c_t/c_f are not straight lines as were the curves of $c_{ht_{\delta f}}$ against c_t/c_f and that K rather than being the slope of the curve (as was k) is the slope of a straight line drawn from $C_{hf_{\delta f}}$ at $\dfrac{c_t}{c_f} = 1.0$ and intersecting the curve at the value of c_t/c_f under consideration.

RESULTS AND DISCUSSION

Correlation of Section Data

Values of c_{ht_α} and $c_{ht_{\delta t}}$.- The results of the correlations of c_{ht_α} (or c_{hf_α}) and $c_{ht_{\delta t}}$ (or $c_{hf_{\delta f}}$) are presented in figure 1 as plots of $c_{ht_{\alpha(\emptyset=0)}}$, $dc_{ht_\alpha}/d\emptyset$, $c_{ht_{\delta t(\emptyset=0)}}$, and $dc_{ht_{\delta t}}/d\emptyset$ against chord ratio c_t/c. The data from which figure 1 was derived were obtained under a variety of conditions; but in all cases the tab and flap gaps were sealed and in most cases the combination of Reynolds number, surface condition, and stream turbulence was such that boundary-layer transition was quite probably located at or ahead of 0.30c. The resulting

scatter of data was such that, in reference 24, the mean
curves from which figure 1 was derived were within ±0.001
of the experimental values of c_{hf_α} and $c_{hf_{\delta f}}$ in most
cases. Although few data were available for the chord
ratios usual for tabs the data in figure 1 should allow
similarly accurate estimations of c_{ht_α}. For $c_{ht_{\delta t}}$,
however, sufficient data were not available for such an
extension, but it is believed that the method of refer-
ence 24 may be used as a guide for additional analysis
as more tab data become available.

Values of $c_{ht_{\delta f}}$.- Values of k required in com-
puting $c_{ht_{\delta f}}$ from equation (3) are presented in figure 2
as plots of k against c_f/c for various trailing-edge
angles and flap and tab-gap conditions. These data show
a considerable amount of scatter; consequently, values
of k for given values of c_f/c and conditions of gaps
were plotted against trailing-edge angle ϕ. From these
cross plots were obtained values of $dk/d\phi$ of 0.00008
for sealed gaps and 0.00022 for open gaps. These values
of $dk/d\phi$ were used to reduce the k-values of figure 2
to zero trailing-edge angle and the resulting data are
plotted in figure 3. The data indicate that as the gaps
at the flap or tab hinges are opened and as the trailing-
edge angle is reduced, the values of k become smaller,
which indicates that the values of $c_{ht_{\delta f}}$ and $c_{hf_{\delta f}}$ more
nearly approach equality. The same trends are illustrated
in figure 4 which presents plots of $c_{ht_{\delta f}}$ against c_t/c_f
for sealed tabs on open and sealed plain 0.30c flaps.
The plots of figure 4 also indicate that a straight line
(constant value of k) represents the data fairly well
for values of c_t/c_f as low as 0.20 with gap sealed even
when the flap is equipped with a pronounced bevel. This
result is typical of the plots derived from pressure-
distribution data.

Correlation of Finite-Span Data

Values of C_{ht_α} and $C_{ht_{\delta t}}$.- The comparisons of
measured values of C_{ht_α} and $C_{ht_{\delta t}}$ with values computed
from equations (4) and (5) are shown in figure 5. The
available data indicate generally satisfactory agreement
between measured and computed values of C_{ht_α}. For $C_{ht_{\delta t}}$,

however, no lifting-surface theory corrections are
available at present and consequently the computed values
are considerably more negative than the measured values
and also show more scatter than do the values of $Ch_{t\alpha}$.

Values of $Ch_{t\delta_f}$.- Values of K (equation (6)) measured
from the finite-span data are plotted against $\overline{c_f'}/c$ in
figure 6. Strictly speaking, the faired line should not
appear on figure 6 since all the test points are not for
the same aspect-ratio. The line is shown however to
indicate more clearly the ranges of K and $\overline{c_f'}/c$ for
which test data exist. Since values of K computed from
section data by lifting-line theory (equation (7)) show a
disagreement with the measured values (fig. 7(a)) there
is evidently an additional lifting-surface-theory correc-
tion, the value of which is as yet unknown. In the
absence of exact values for such corrections the differ-
ences between the computed and measured values of K were
plotted against aspect-ratio, and an empirical correction
of $\Delta K = 0.0025$ $(A - 4.5)$ was derived. This ΔK should
be added to the value of K computed by lifting-line
theory (equation (7)). The resulting equation is

$$K = k + \frac{\dfrac{A}{AE + 2}}{\left(1 - \dfrac{\overline{c_t}}{\overline{c_f}}\right)} \alpha_{\delta f} \left(ch_{t\alpha} - ch_{f\alpha}\right) + 0.0025 \ (A - 4.5) \quad (8)$$

Values of K computed from equation (8) are plotted
against measured values of K in figure 7(b). In this
case the agreement is improved and it is thus believed
that equation (8) presents a correction for K that is
acceptable until more complete lifting-surface-theory
computations are made or until more finite-span tab data
become available for use in deriving a better empirical
correction.

Effects of Mach Number

At present very few data are available to show the
effects of Mach number and Reynolds number on tab hinge-
moment characteristics. Some information, however, has
been obtained from pressure-distribution data presented

in reference 17. Increments in c_{ht_α} caused by an
increase in Mach number from 0.197 to 0.472 for plain
sealed tabs on 0.20c open-gap balanced flaps on
NACA 66(215)-216 and NACA 23012 airfoils are shown in
figure 8. These data indicate slightly more negative
increments in c_{ht_α} as the tab chord is reduced and
considerably more negative increments as the trailing-
edge angle is reduced for this particular case where there
were open gaps through the airfoils some distance ahead
of the tab hinge lines.

Values of the tab section hinge-moment constant k
derived from the pressure-distribution data of refer-
ence 17 are presented in figure 9. These data indicate
a decrease in k as the Mach number is increased with
the greatest decrease in k occurring for the sealed
internal-balance flap on the NACA 66(215)-216 airfoil.

CONCLUDING REMARKS

The analysis of available tab hinge-moment data
obtained in two- and three-dimensional force tests and
in two-dimensional pressure-distribution tests indicated
that present methods of estimating the rate of change of
flap section hinge-moment coefficient with angle of attack
and with flap deflection could be extended, over small
ranges of angle of attack and flap deflection, to chord
ratios small enough to include the rate of change of tab
section hinge-moment coefficient with angle of attack.
Indications are that the method can be extended to include
the rate of change of tab section hinge-moment coefficient
with tab deflection when more tab data are available. The
analysis indicated that available lifting-surface theory
corrections for the rate of change of tab hinge-moment
coefficient with angle of attack will allow reasonable
accuracy in converting section data to finite-span data.
With regard to the rates of change of tab hinge-moment
coefficient with tab deflection and with flap deflection,
however, either lifting-surface computations should be
made or more data should be obtained in order that cor-
rections (either theoretical or empirical) may be derived
for these derivatives. Some data are available and have
been presented concerning Mach number effects on tab hinge
moments but they are so limited as to be practically use-
less for design purposes; consequently, it appears quite

desirable to obtain more tab hinge-moment data at large ✓
values of Mach number.

Langley Memorial Aeronautical Laboratory
    National Advisory Committee for Aeronautics
        Langley Field, Va.

REFERENCES

1. Rogallo, F. M.: Collection of Balanced-Aileron Test
      Data. NACA ACR No. 4A11, 1944.

2. Sears, Richard I.: Wind-Tunnel Data on the Aerodynamic
      Characteristics of Airplane Control Surfaces.
      NACA ACR No. 3L08, 1943.

3. Rogallo, F. M., and Lowry, John G.: Résumé of Data
      for Internally Balanced Ailerons. NACA RB, March
      1943.

4. Purser, Paul E., and Toll, Thomas A.: Analysis of
      Available Data on Control Surfaces Having Plain-
      Overhang and Frise Balances. NACA ACR No. L4E13,
      1944.

5. Purser, Paul E., and Gillis, Clarence L.: Preliminary
      Correlation of the Effects of Beveled Trailing Edges
      on the Hinge-Moment Characteristics of Control Sur-
      faces. NACA CB No. 3E14, 1943.

6. Lowry, John G.: Résumé of Hinge-Moment Data for
      Unshielded Horn-Balanced Control Surfaces. NACA RB
      No. 3F19, 1943.

7. Lowry, John G., Maloney, James A., and Garner,
      I. Elizabeth: Wind-Tunnel Investigation of Shielded
      Horn Balances and Tabs on a 0.7-Scale Model of
      XF6F Vertical Tail Surface. NACA ACR No. 4C11,
      1944.

8. Crandall, Stewart M., and Murray, Harry E.: Analysis
      of Available Data on the Effects of Tabs on Control-
      Surface Hinge Moments. NACA TN No. 1049, 1946.

9. Swanson, Robert S., and Crandall, Stewart M.: Analysis
      of Available Data on the Effectiveness of Ailerons
      without Exposed Overhang Balance. NACA ACR
      No. L4E01, 1944.

10. Phillips, William H.: Application of Spring Tabs to
      Elevator Controls. NACA ARR No. L4H28, 1944.

11. Phillips, William H.: The Use of Geared Spring Tabs
      for Elevator Control. NACA RB No. L5A13, 1945.

12. Jones, Robert T.: Correction of the Lifting-Line
    Theory for the Effect of the Chord. NACA TN
    No. 817, 1941.

13. Street, William G., and Ames, Milton B., Jr.:
    Pressure-Distribution Investigation of an
    N.A.C.A. 0009 Airfoil with a 50-Percent-Chord
    Plain Flap and Three Tabs. NACA TN No. 734, 1939.

14. Ames, Milton B., Jr., and Sears, Richard I.: Pressure-
    Distribution Investigation of an N.A.C.A. 0009 Air-
    foil with a 30-Percent-Chord Plain Flap and Three
    Tabs. NACA TN No. 759, 1940.

15. Ames, Milton B., Jr., and Sears, Richard I.: Pressure-
    Distribution Investigation of an N.A.C.A. 0009 Air-
    foil with an 80-Percent-Chord Plain Flap and Three
    Tabs. NACA TN No. 761, 1940.

16. Ames, Milton B., Jr., and Sears, Richard I.: Determi-
    nation of Control-Surface Characteristics from
    NACA Plain-Flap and Tab Data. NACA Rep. No. 721,
    1941.

17. Letko, W., and Denaci, H. G.: Wind Tunnel Tests of
    Ailerons at Various Speeds. V - Pressure Distri-
    butions over the NACA 66,2-216 and NACA 23012 Air-
    foils with Various Balances on 0.20-Chord Ailerons.
    NACA ACR No. 3K05, 1943.

18. Hoggard, H. Page, Jr., and Bulloch, Majorie E.: Wind-
    Tunnel Investigation of Control-Surface Character-
    istics. XVI - Pressure Distribution over an
    NACA 0009 Airfoil with 0.30-Airfoil-Chord Beveled
    Trailing-Edge Flaps. NACA ARR No. L4D03, 1944.

19. Holtzclaw, Ralph W., and Crane, Robert M.: Wind-
    Tunnel Investigation of Ailerons on a Low-Drag
    Airfoil. III - The Effect of Tabs. NACA ACR
    No. 4H15, 1944.

20. Sears, Richard I.: Wind-Tunnel Investigation of
    Control Surface Characteristics. I - Effect of
    Gap on the Aerodynamic Characteristics of an
    NACA 0009 Airfoil with a 30-Percent-Chord Plain
    Flap. NACA ARR, June 1941.

21. Sears, Richard I., and Liddell, Robert B.:   Wind-
    Tunnel Investigation of Control-Surface Character-
    istics.   VI - A 30-Percent-Chord Plain Flap on the
    NACA 0015 Airfoil.   NACA ARR, June 1942.

22. Sears, Richard I., and Purser, Paul E.:   Wind-Tunnel
    Investigation of Control-Surface Characteristics.
    XIV - NACA 0009 Airfoil with a 20-Percent-Chord
    Double Plain Flap.   NACA ARR No. 3F29, 1943.

23. Gillis, Clarence L., and Lockwood, Vernard E.:   Wind-
    Tunnel Investigation of Control-Surface Character-
    istics.   XIII - Various Flap Overhangs Used with
    a 30-Percent-Chord Flap on an NACA 66-009 Airfoil.
    NACA ACR No. 3G20, 1943.

24. Research Department: Summary of Lateral Control
    Research.   Compiled by Thomas A. Toll.   NACA TN
    No. 1245, 1947.

25. Glauert, H.:   Theoretical Relationships for an Aerofoil
    with Hinged Flap.   R.   & M. No. 1095, British A.R.C.,
    1927.

26. Perring, W. G. A.:   The Theoretical Relationships for
    an Aerofoil with a Multiply Hinged Flap System.
    R. & M. No. 1171, British A.R.C., 1928.

27. Swanson, Robert S., and Priddy, E. LaVerne: Lifting-
    Surface-Theory Values of the Damping in Roll and
    of the Parameter Used in Estimating Aileron Stick
    Forces.   NACA ARR No. L5F23, 1945.

TABLE I.- INFORMATION REGARDING PRESSURE-DISTRIBUTION-TEST
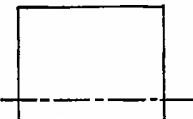
MODELS IN TWO-DIMENSIONAL FLOW

Model	Symbol	Plan form	Airfoil section	∅ (deg)	c_t/c	Tab gap	c_f/c	Flap gap	Air-flow characteristics	Published reference
1	⊙		NACA 0009	11.6	0 to 0.50	0	0.10 to 0.50	0	R = 1.77 × 10⁶ M = 0.09 τ = 1.93	13 to 16
2	⊙̸		NACA 66(215)-216	9.3	0 to 0.20	0	0.20	0 and 0.0055c	R = 2.8 × 10⁶ to 6.7 × 10⁶ M = 0.20 to 0.47 $\tau \longrightarrow 1.00$	17
3	⊘		NACA 23012	15.5	0 to 0.20	0	0.20	0.0055c	R = 2.8 × 10⁶ to 6.7 × 10⁶ M = 0.20 to 0.47 $\tau \longrightarrow 1.00$	17
4	⊙̍		NACA 6-series	11.0	0 to 0.225	0	0.225	0.0050c	R = 6.0 × 10⁶ M = 0.14 $\tau \longrightarrow 1.00$	---------
5	△		NACA 0009	25.4 and 30.5	0 to 0.30	0	0.30	0 and 0.0050c	R = 2.76 × 10⁶ M = 0.10 τ = 1.93	18

NATIONAL ADVISORY
COMMITTEE FOR AERONAUTICS

TABLE II.- INFORMATION REGARDING FORCE-TEST MODELS IN

TWO-DIMENSIONAL FLOW

Model	Symbol	Plan form	Airfoil section	β (deg)	c_t/c_f	Tab gap	c_f/c	Flap gap	$c_{h_{\delta_f}}$	$c_{h_{t_{\delta_f}}}$	$c_{T_{t_{\delta_t}}}$	$c_{h_{t_\alpha}}$	Air-flow characteristics	Published reference
6			NACA 65,3-018	25.0	0.25	0	0.18	0	a-0.0049	0.0020	-0.0022	0.0054	R = 2.8 x 10^6 and 5.1 x 10^6 M = 0.20 and M = 0.38 T→1.00	---------
7			NACA 66(215)216 a = 0.6	9.3 21.7	0.20 .20	0.0008c .0008c	0.20 .20	0 0	-0.0096 -.0050	-0.0044 .0010	-0.0074 -.0039	-0.0028 .0024	R = 9.0 x 10^6 M = 0.32 R = 9.0 x 10^6 M = 0.32 T→1.00	19
8			NACA 0009	11.6 11.6	0.20 .20	0.0010c .0010c	0.30 .30	0.0010c 0	-0.0115 -.0125	-0.0035 -.0035	-0.0061 -.0070	-0.0009 -.0015	R = 2.76 x 10^6 M = 0.10 T = 1.93	20
9			NACA 0015	19.7	0.20	0	0.30	0	-0.0080	-0.0010	-0.0052	0.0012	R = 2.76 x 10^6 M = 0.10 T = 1.93	21
10			NACA 0009	11.6	0.75	0	0.20	0	-0.0100	-0.0075	-0.0060	-0.0033	F = 2.76 x 10^6 M = 0.10 T = 1.93	22
11			NACA 66-009	7.4	0.20	0.0010c	0.30	0.0050c	-0.0128	-0.0056	-0.0100	-0.0046	R = 2.76 x 10^6 M = 0.10 T = 1.93	23
12			NACA 0012 (modified)	10.0	0.20	0.0040c	0.40	0.0030c	a-0.0120	-0.0024	-0.0089	-0.0024	R = 6.0 x 10^6 M = 0.14 T = 1.00	---------

a Plain flap value estimated from balanced-flap tests.

TABLE III - INFORMATION REGARDING FORCE-TEST MODELS IN

THREE-DIMENSIONAL FLOW

Model	Symbol	Plan form	Airfoil section Root	Airfoil section Tip	$\overline{\Lambda}$ (deg)	A	λ	Tab location $\frac{y_1}{b/2}$	Tab location $\frac{y_a}{b/2}$	c_t/c_f	Tab gap	c_f/c	Flap gap	$C_{h_{f_{\delta_f}}}$	$C_{h_{t_{\delta_f}}}$	$C_{h_{t_{\delta_t}}}$	$C_{h_{t_a}}$	Air-flow characteristics	Published reference
13	◇		18-percent thick conventional	9-percent thick conventional	16.5	6.86	0.625	0.14	0.41	0.375	0	0.167	0.0025c	[a]-0.0060	0.0030	-------	0.0011	R = 4.0 × 10⁶ M = 0.30 T→1.00	---------
14	◇ ◇ ◇ ◇		NACA 0014	NACA 0014	16.0 16.0 16.0 16.0	4.06 4.06 4.06 4.06	1.000 1.000 1.000 1.000	0 0 0 0	0.39 .40 .59 .59	0.408 .395 .395 .408	0 .0062c .0062c .0062c	0.311 .322 .322 .311	0 .0062c .0062c .0062c	[a]-0.0091 [a]-.0062 [a]-.0087 [a]-.0080	-0.0015 -.0050 -.0043 -.0014	-0.0050 -.0040 -.0068 -.0065	-0.0003 -.0028 -.0015 -.0018	R = 1.67 × 10⁶ M = 0.10 T = 1.6	---------
15	△ ▽ ▷ ◁		Modified NACA 16-series	Modified NACA 16-series	11.5 11.5 11.5 11.5	2.86 2.86 2.86 2.86	0.392 .392 .392 .392	0.34 .34 .34 .34	0.56 .56 .56 .56	[b]0.303 [b].303 [c].303 [c].303	0.0015c 0 .0015c 0	0.320 .320 .320 .320	0 0 0 0	-0.0080 -.0086 -.0086 -.0097	-0.0010 -.0011 -.0015 -.0014	-0.0064 -.0063 -.0052 -.0030	0 0 -0.0003 0	R = 2.30 × 10⁶ M = 0.10 T = 1.6	7
16	▽ ◁		Modified NACA 65₁-012	Modified NACA 65₁-012	16.0 16.0	5.00 5.00	0.500 .500	0.09 .09	0.45 .45	0.200 .200	0.0010c .0010c	0.320 .320	0 0	[a]-0.0119 [a]-.0151	-0.0019 -.0019	-0.0055 -.0065	0 0.0008	R = 2.76 × 10⁶ M = 0.21 T→1.00 transition free transition fixed at 0.25c	---------
17	◁		NACA 0015	NACA 0009	16.7	4.50	0.500	0.12	0.65	0.200	Open min. gap	0.410	0	-0.0062	-0.0003	-------	0.0005	R = 4.00 × 10⁶ M = 0.08 T→1.00	---------
18	⊡ ⊍		Modified NACA 66-series	Modified NACA 66-series	15.0 15.0	2.41 2.41	0.47 .47	0.52 .52	0.58 .58	0.325 .325	0.0015c 0	0.325 .325	0.0033c 0	-0.0045 -.0045	-0.0010 -.0014	-0.0060 -------	0.0007 .0005	R = 1.51 × 10⁶ M = 0.10 T = 1.6	---------

[a]Plain-flap value estimated from balanced-flap tests.

[b]Tab-hinge:

[c]Tab-hinge:
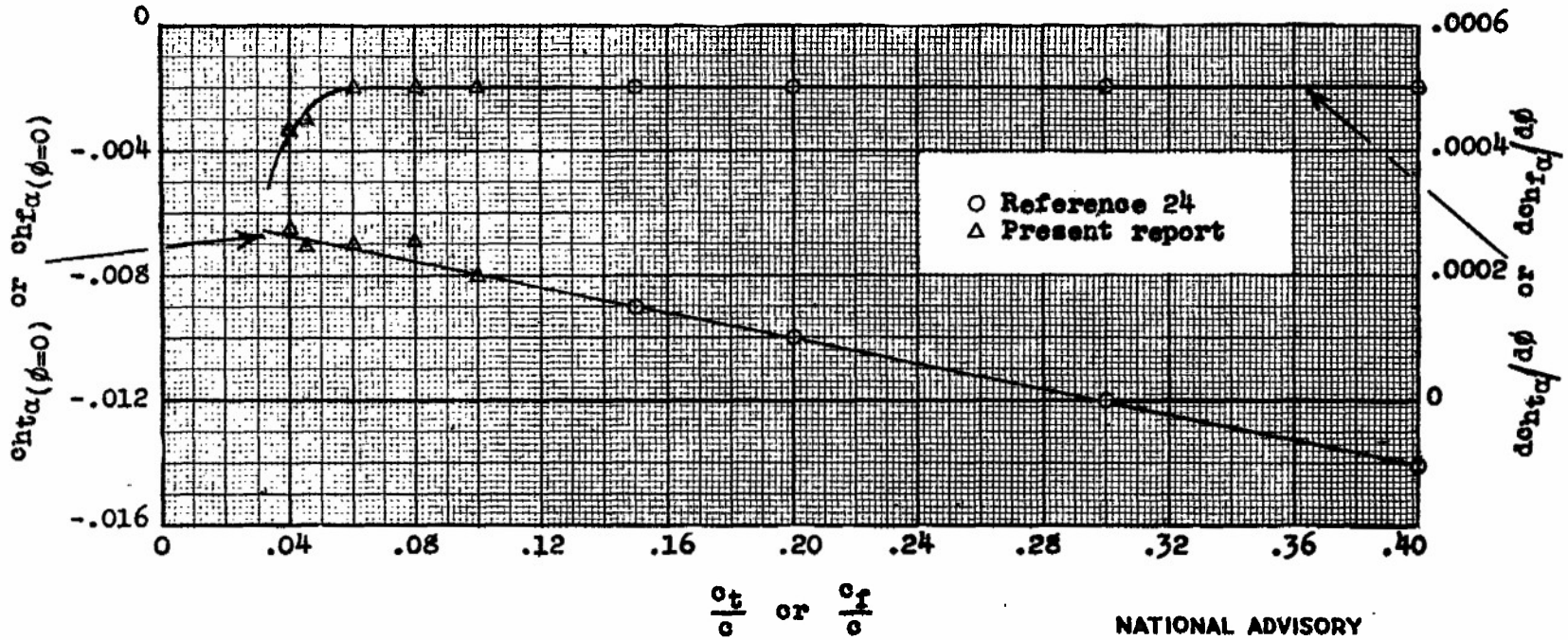
(a) Angle-of-attack slopes.

Figure 1.- Effect of tab or flap chord on the hinge-moment parameters derived from various two-dimensional pressure-distribution and force-test data.
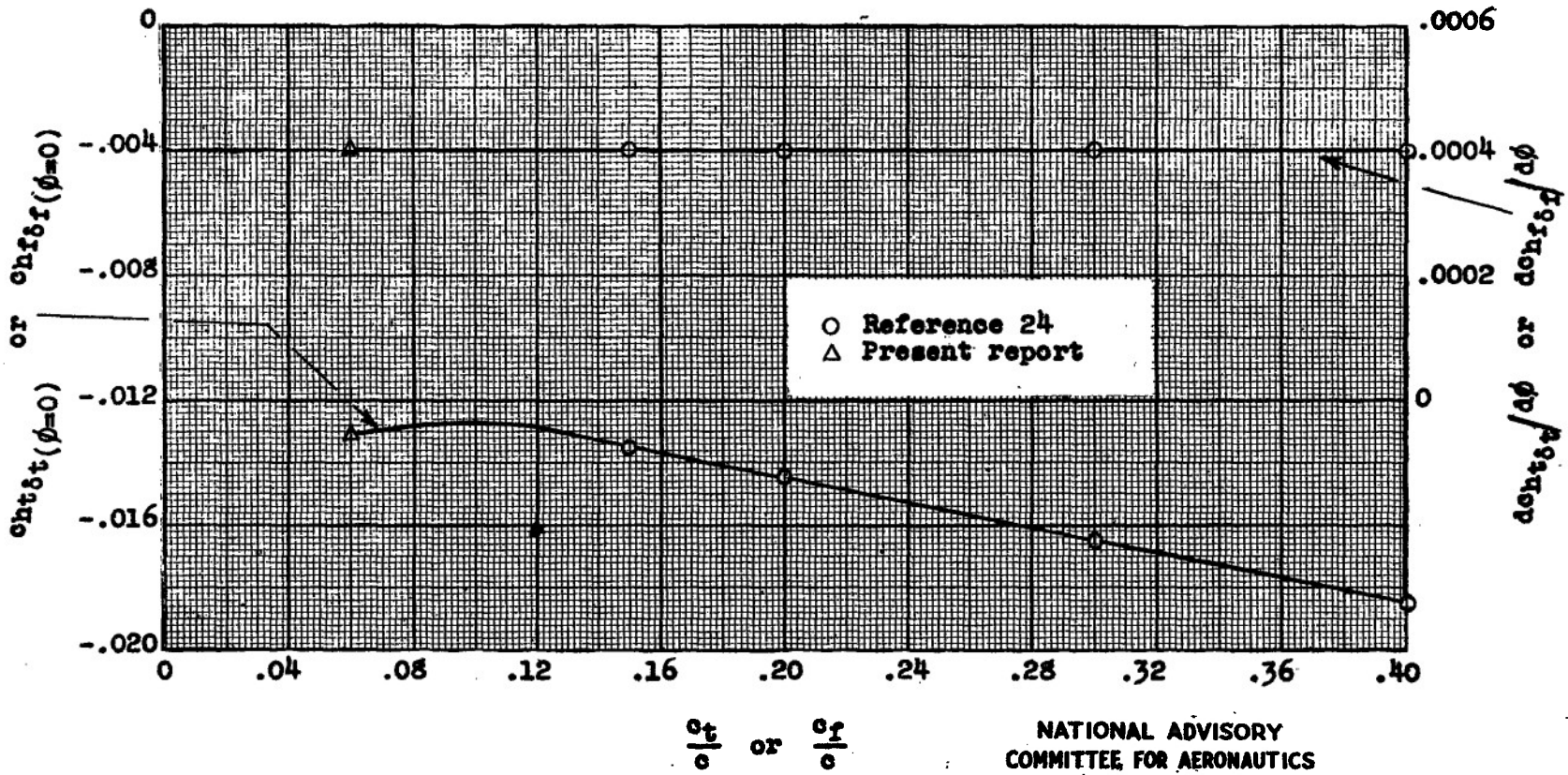
(b) Tab or flap-deflection slopes.
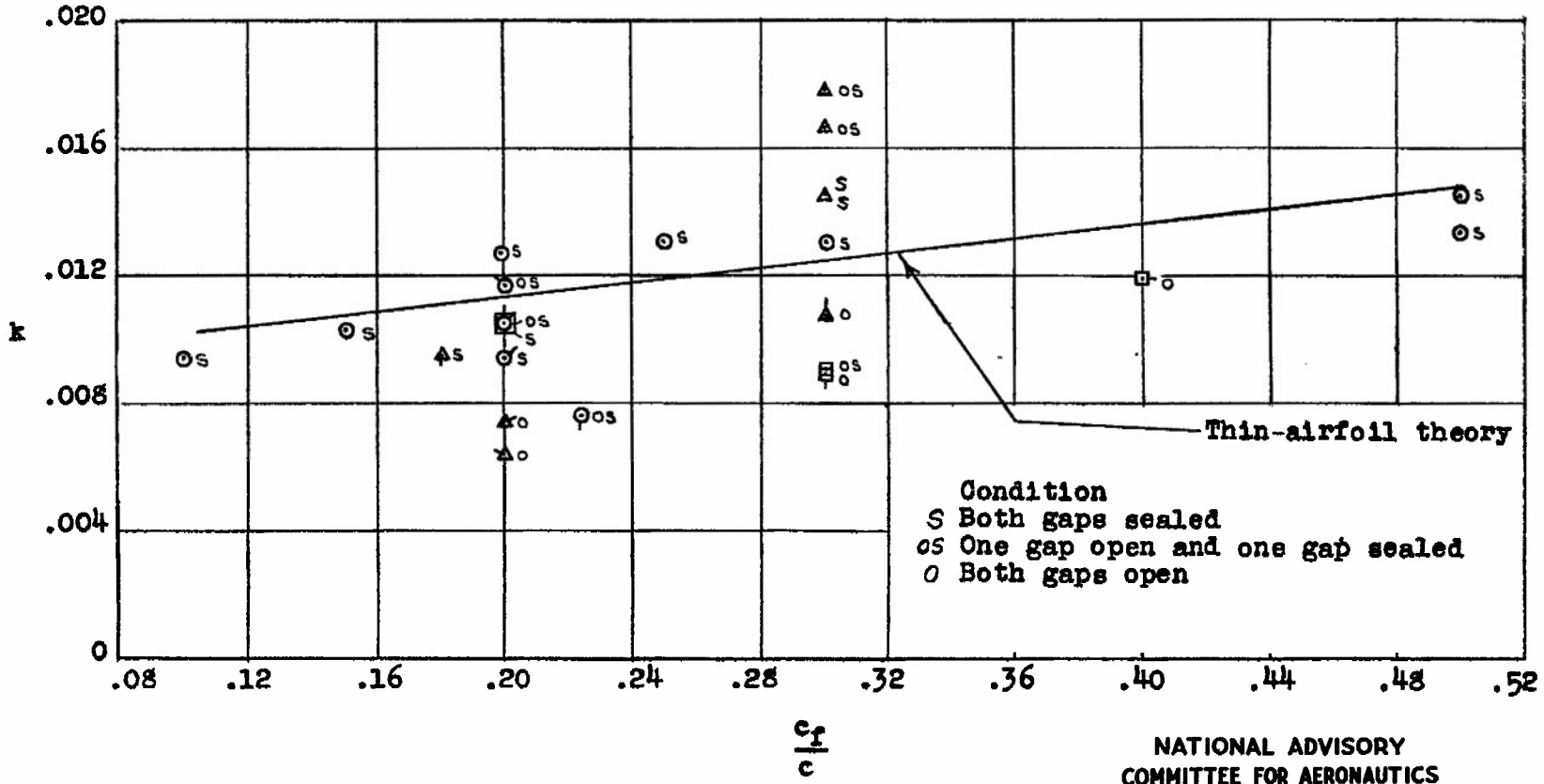
Figure 1.- Concluded.

Fig. 2

Figure 2.- Variation of tab section hinge-moment constant k with flap chord ratio $\frac{c_f}{c}$ for various combinations of flap and tab gap. Symbols refer to models listed in tables I and II.
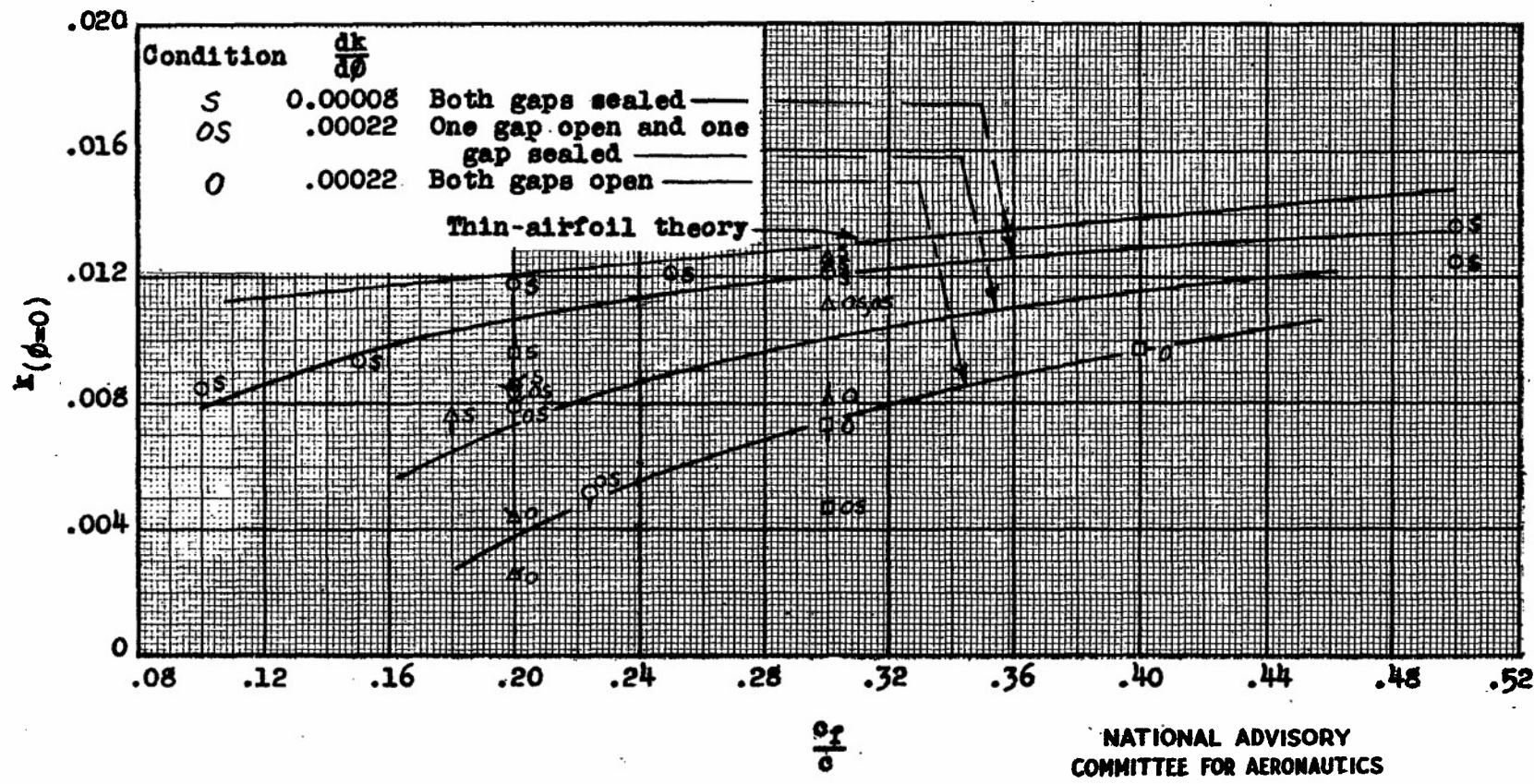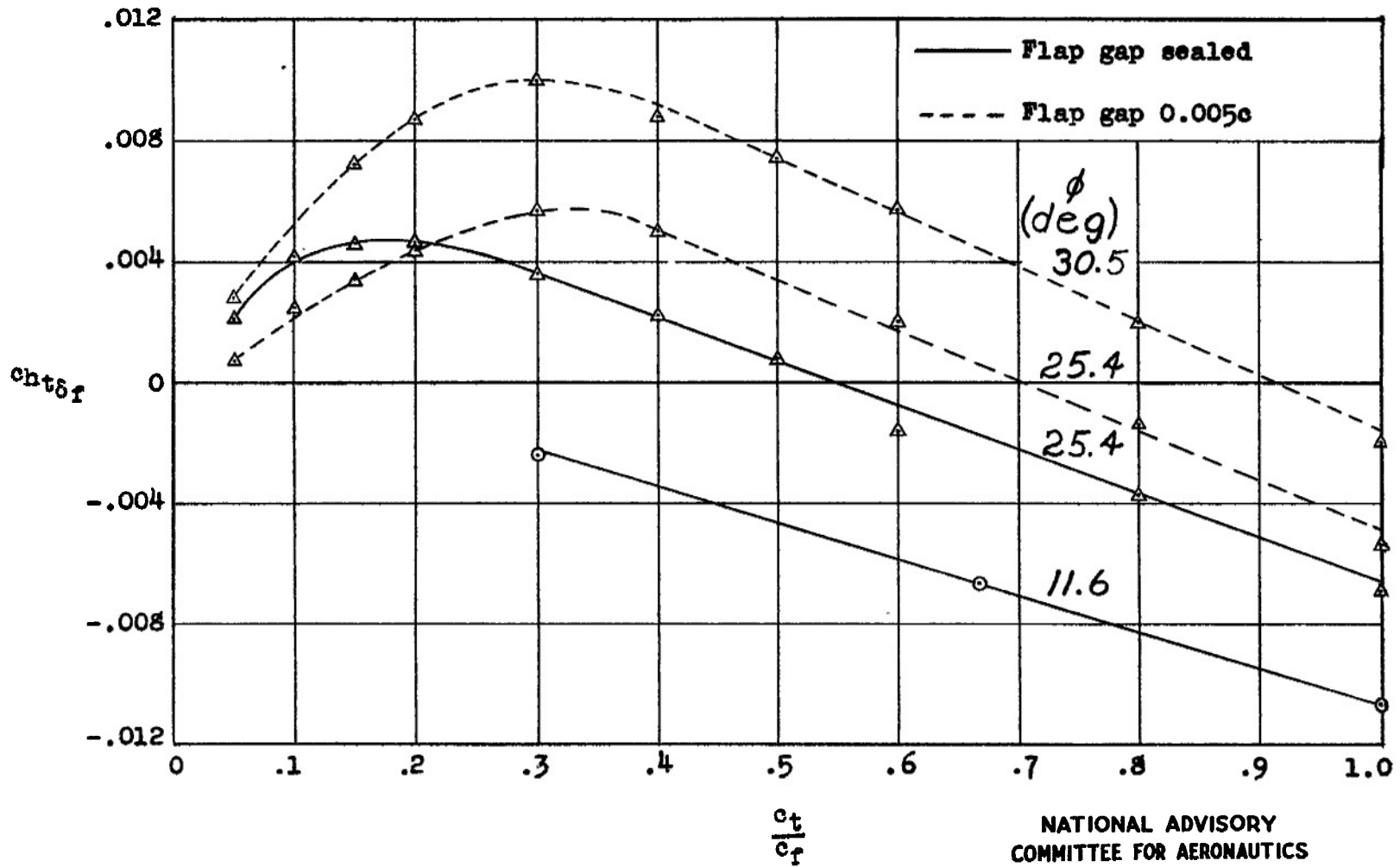
Figure 3.- Variation of tab section hinge-moment constant at 0° trailing-edge angle $k(\phi=0)$ with flap-chord ratio $\frac{c_f}{c}$ for various combinations of flap and tab gap. Symbols refer to models listed in tables I and II.

Fig. 3

Fig. 4

Figure 4.- Effect of trailing-edge angle ϕ on the variation of $c_{h_{t_{\delta f}}}$ with $\dfrac{c_t}{c_f}$ for plain sealed- and open-gap 0.30c flaps on an NACA 0009 airfoil section. Symbols refer to models listed in table I.
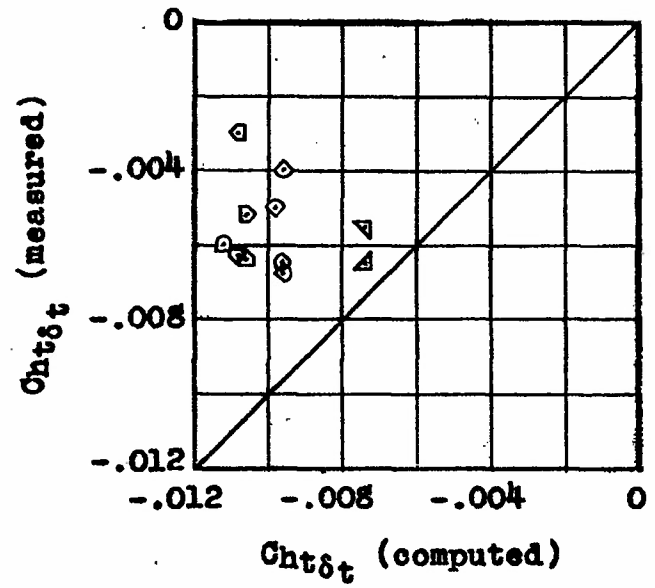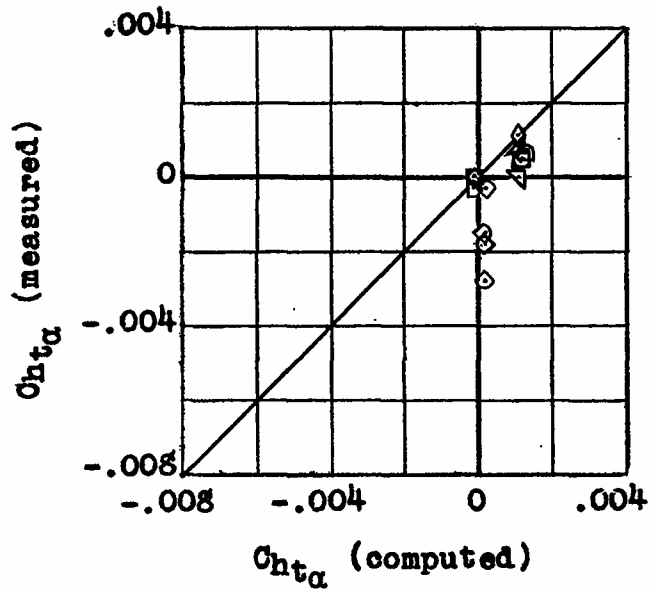
Figure 5.- Comparison of measured and computed values of $C_{h t_\alpha}$ and $C_{h t_{\delta_t}}$. Symbols refer to models in table III.

Fig. 5

Fig. 6
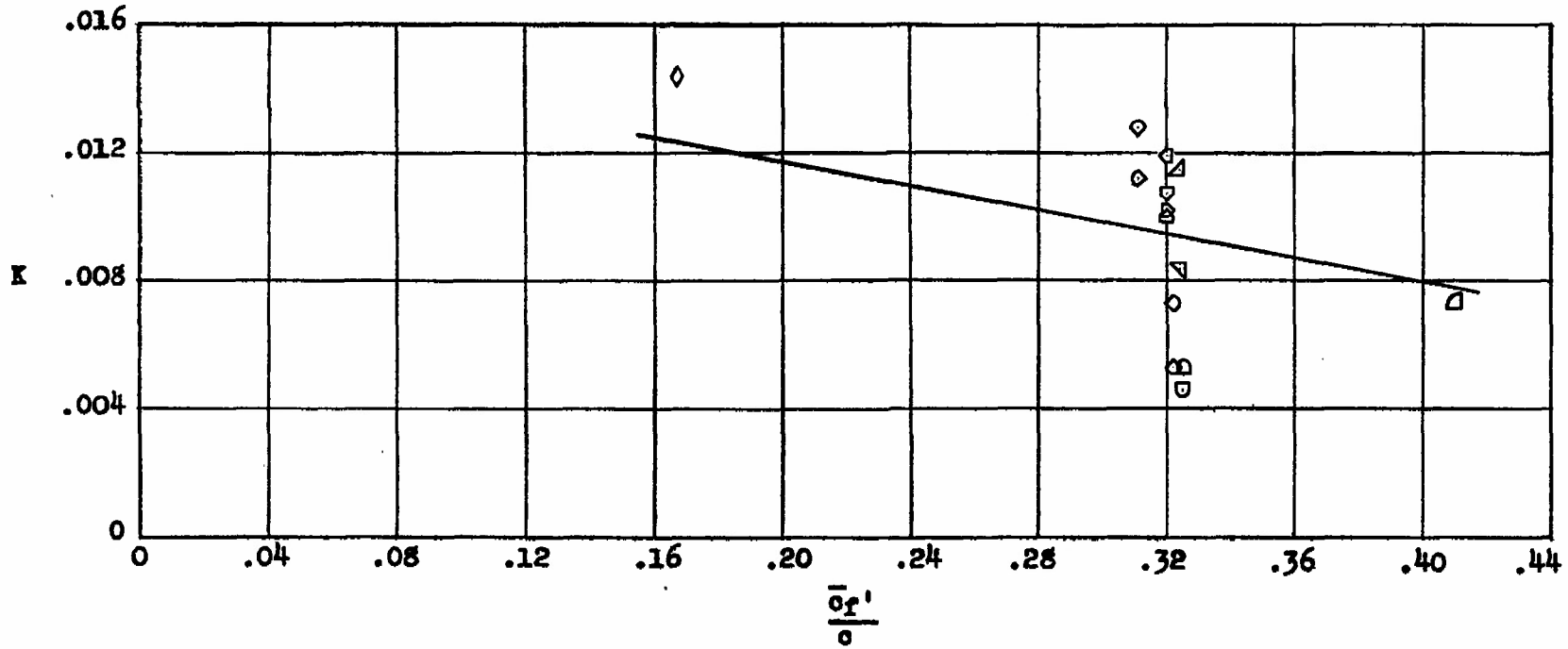
Figure 6.- Measured values of finite-span tab hinge-moment constant K plotted against flap-chord ratio $\dfrac{\overline{c_f}'}{c}$ for illustrative purposes only. Symbols refer to models in table III.

NATIONAL ADVISORY
COMMITTEE FOR AERONAUTICS
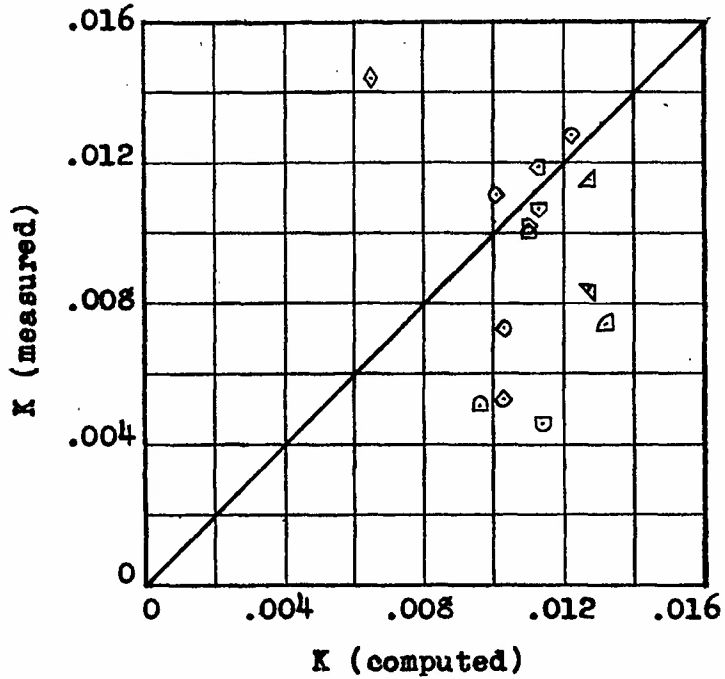
(a) Lifting-line theory (equation (7)).
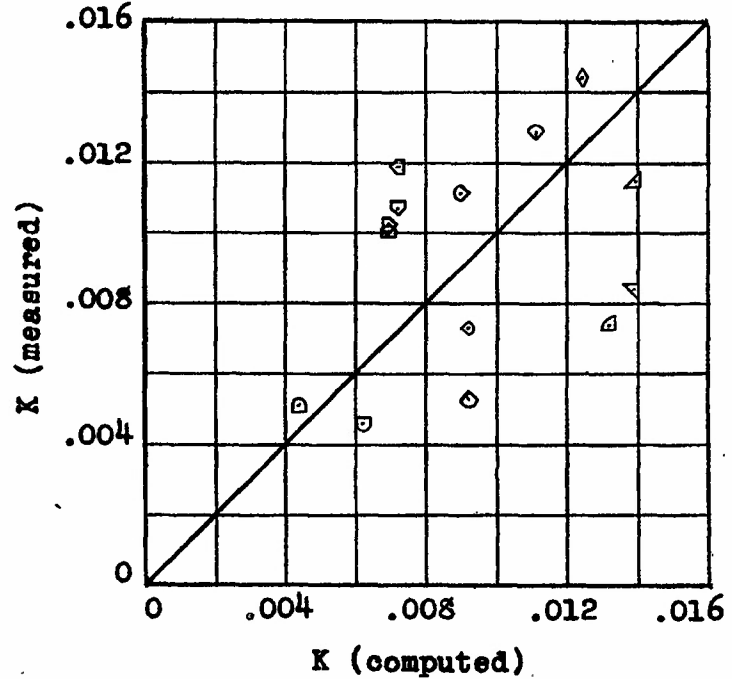
(b) Lifting-line theory plus empirical correction (equation (8)).

Figure 7.- Comparison of measured and computed values of the finite-span tab hinge-moment constant K. Symbols refer to models in table III.
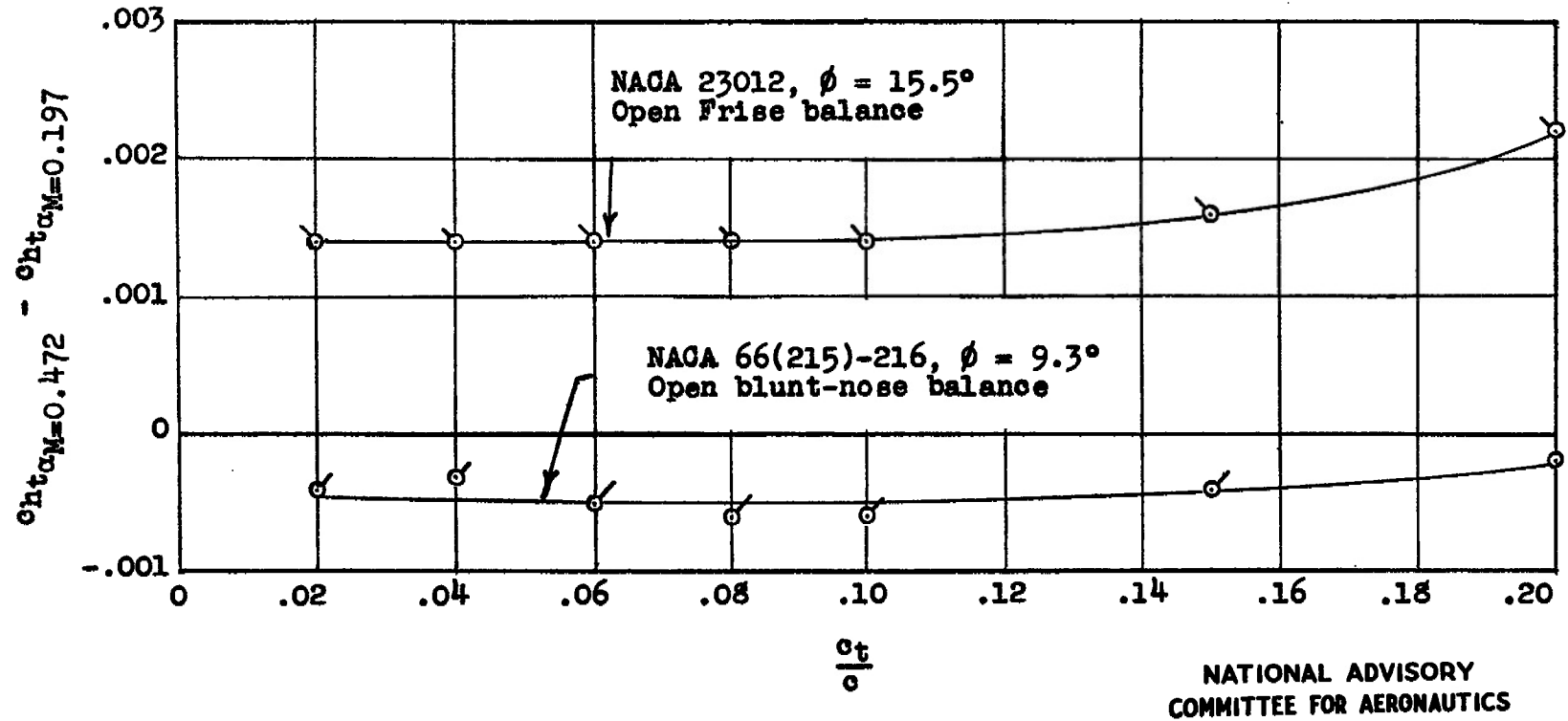
NATIONAL ADVISORY
COMMITTEE FOR AERONAUTICS

Fig. 7

Fig. 8

Figure 8.- Effect of tab-chord ratio on the increment in c_{ht_α} resulting from an increase in Mach number for plain sealed tabs on 0.20c open-gap balanced flaps on NACA 23012 and NACA 66(215)-216 airfoils. Derived from pressure-distribution data of reference 17. R, 2.8 x 10^6 for M = 0.197; R, 6.7 x 10^6 for M = 0.472.
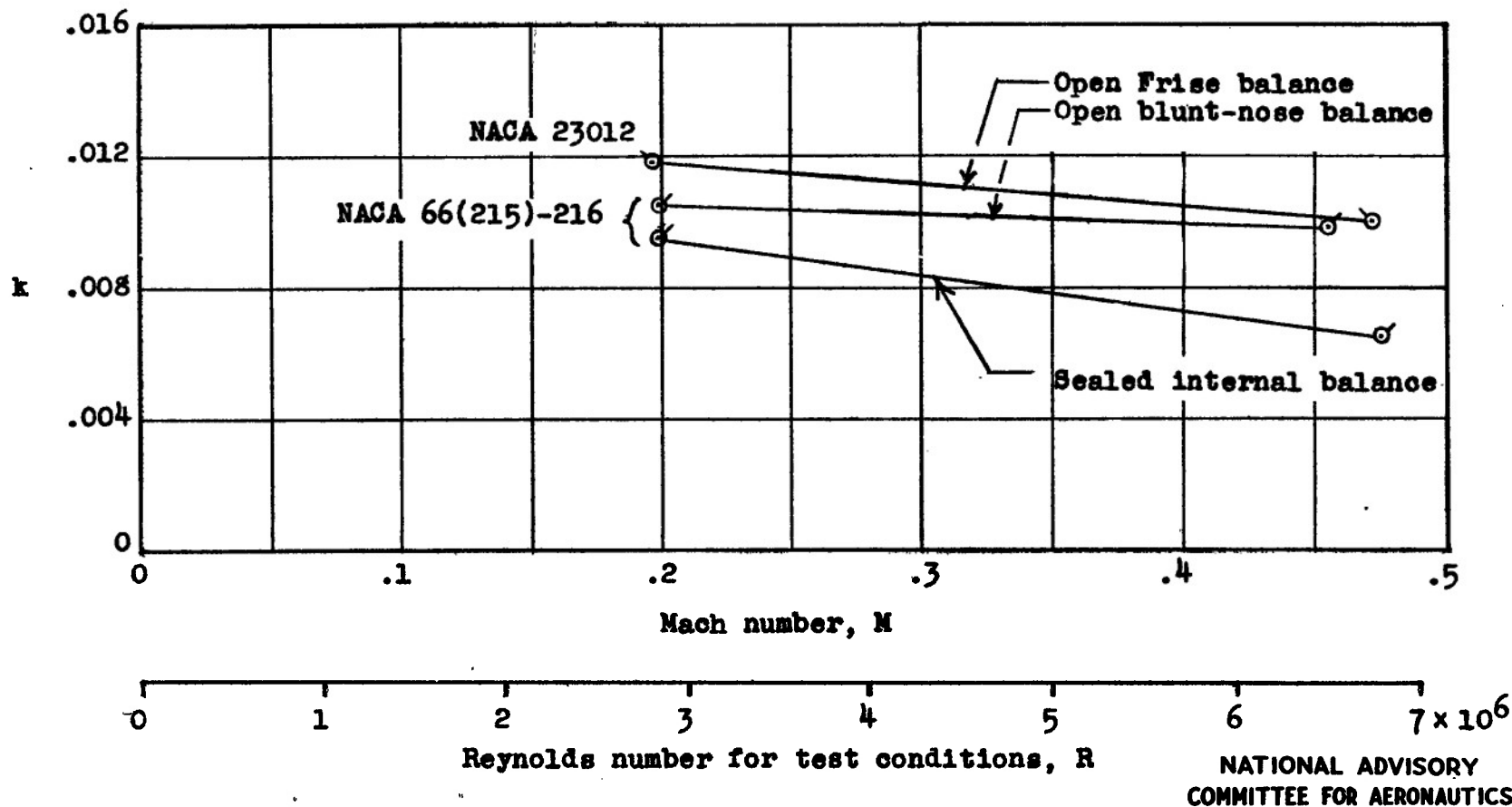
Figure 9.- Variation of section tab hinge-moment constant k with Mach number and Reynolds number for 0.20c flaps on NACA 66(215)-216 and NACA 23012 airfoil sections. Symbols refer to models listed in table I.

Fig. 9

				ATI- 8364
				REVISION (None)
				ORIG. AGENCY NO. TN-1113
				PUBLISHING AGENCY NO. (Same)

TITLE: Collection and Analysis of Hinge-Moment Data on Control-Surface Tabs

AUTHOR(S): Purser, Paul E.; Cook, Charles B.
ORIGINATING AGENCY: Langley Memorial Aeronautical Laboratory, Langley Field, Va.
PUBLISHED BY: National Advisory Committee for Aeronautics, Washington, D. C.

DATE	DOC. CLASS.	COUNTRY	LANGUAGE	PAGES	ILLUSTRATIONS
April '47	Restr.	U.S.	Eng.	31	tables, graphs

ABSTRACT:

Hinge-moment data, all of which are for plain unbalanced tabs, were obtained from force tests of models in two- and three-dimensional flow pressure-distribution measurements on model in two-dimensional flow. Data available were not sufficient to allow accurate determinations of all various factors affecting difference between section and finite span values of tab hinge-moment parameters; desirability is indicated of obtaining more tab hinge-moment data on finite-span models at large values of Mach numbers and obtaining more complete aspect-ratio corrections to tab hinge-moment characteristics.

EO .0501 aa 5 NoV 1353

AD-B805 965

Publishing Agency

(25)

* Aerodynamic Control Surfaces
Moments